Jundishapur J Health Sci. 2022 April; 14(2):e122840. doi: 10.5812/jjhs.122840.

Published online 2022 April 3. **Research Article**

Removal of Heavy Metal Ions from Water Using Functionalized Carbon Nanosheet: A Density-Functional Theory Study

Leila Javarani [1], Mohammad Malakootian [2, 3], Amir Hessam Hassani [1, *] and Amir Hossein Javid [4]

[1] Department of Natural Resources and Environment, Science and Research Branch, Islamic Azad University, Tehran, Iran
[2] Environmental Health Engineering Research Center, Kerman University of Medical Sciences, Kerman, Iran
[3] Department of Environmental Health Engineering, School of Public Health, Kerman University of Medical Sciences, Kerman, Iran
[4] Department of Environmental Engineering, Science and Research Branch, Islamic Azad University, Tehran, Iran

[*] *Corresponding author*: Department of Natural Resources and Environment, Science and Research Branch, Islamic Azad university, Tehran, Iran. Email: ahhi1346@gmail.com

Received 2022 January 22; **Revised** 2022 February 19; **Accepted** 2022 March 05.

Abstract

Background: Currently, a clean environment and human health have been regarded as the most important challenges of humankind; therefore, the ability of carbon-based nanomaterials as a new type of adsorbents in the removal of various pollutants from aqueous solutions has caused the widespread attention of research groups.

Objectives: Carbon nanosheet (CNS) and its amine-functionalized derivatives were considered to remove heavy metal ions (HMIs) (zinc(II) ion [Zn^{2+}]/cadmium(II) ion [Cd^{2+}]/mercury(II) ion [Hg^{2+}]) from water.

Methods: This theoretical study in the framework of density-functional theory (DFT) was performed to gain insight into the HMIs (Zn^{2+}/Cd^{2+}/Hg^{2+}) adsorption and removal by CNS and {$(NH_2)_n$-CNS (n = 1 - 2)}. The calculation level was hybrid DFT methods, such as wB97XD/lanl2dz.

Results: Based on DFT calculations, more negative chemical potential value (-1.827 eV), high global softness (0.964 eV), low highest occupied molecular orbital $(NH_2)_2$-CNS lowest unoccupied molecular orbital-HMI gap, and more negative adsorption energy (range: -75 to -93 kJ mol^{-1}) in $(NH_2)_2$-CNS demonstrated that this compound as a suitable adsorbent removed HMIs (Zn^{2+}/Cd^{2+}/Hg^{2+}) from water than other nanosheets. The HMIs adsorption was confirmed by the natural bond orbital and quantum theory of atoms in molecules.

Conclusions: The CNS and amine-functionalized structures have a good ability for HMIs (Zn^{2+}/Cd^{2+}/Hg^{2+}) removal due to high chemical potential, electrophilicity, and adsorption energy.

Keywords: Water Contaminations, Heavy Metals, Density-Functional Theory, Carbon Nanosheet, Electrostatic Interactions

1. Background

Currently, maintaining a clean environment has become one of the essential tasks of humankind. In general, the inattention to pollution particles of the environment and living organisms is naturally followed by numerous environmental problems, diseases, and cancers. A part of these pollution particles exists in water, such as toxic and heavy metals (metal ions) in water and/or wastewater. The increasing rate of environmental problems in numerous societies has made it necessary for research groups to put forward new and logical solutions for this issue. Therefore, the current study focused on proposing a new method to remove heavy metal ions (HMIs) from water and/or wastewater.

The removal of HMIs as one of the pollution sources in seawater or industrial wastewater needs to adsorb on large surface areas and high active sites (1-20). Therefore, nanostructures with these properties are introduced as excellent candidates (1, 21). For example, nanostructures with a good ability of adsorption were introduced to remove heavy metal atoms (1). In another theoretical study, graphene-based materials were introduced for the adsorptive removal of pollutants, such as HMIs, from water (21). For instance, amine-functionalized graphene oxide was used as a sorbent to achieve carbon dioxide capture (21). Therefore, theoretical studies can help to the precise understanding of the interaction between nanostructures and HMIs. This theoretical study proposes logical methods to experimental research groups for the removal of pollution particles.

2. Objectives

The existence of HMIs (zinc(II) ion [Zn^{2+}]/cadmium(II) ion [Cd^{2+}]/mercury(II) ion [Hg^{2+}]) in seawater or wastewater results in numerous environmental problems, dis-

eases, and cancers. Therefore, the natural removal of HMIs is followed by decreasing the aforementioned problems. The major objective of this study was to investigate the adsorption of HMIs (Zn^{2+}/Cd^{2+}/Hg^{2+}) in zigzag nanosheets (NSs), such as functionalized carbon nanosheet (CNS) {$(NH_2)_n$-CNS (n = 1 - 2)}, using density-functional theory (DFT). The HMIs are susceptible to binding to {$(NH_2)_n$-CNS (n = 1 - 2)} structures. Therefore, the present study will optimize CNS {$(NH_2)_n$-CNS (n = 1 - 2)} structures and their complexes with HMIs (Zn^{2+}/Cd^{2+}/Hg^{2+}) to obtain their ground states. In addition, the quantum theory of atoms in molecules (QTAIM) and natural bond orbital (NBO) analysis confirm the formed bonds and interactions between {$(NH_2)_n$-CNS (n = 1 - 2)} structures and HMIs (Zn^{2+}/Cd^{2+}/Hg^{2+}) in the best configuration and orientation.

3. Methods

The methodological approach in this study was based on quantum mechanics studies. The advantage of these methods is gaining insight into CNS and {$(NH_2)_n$-CNS (n = 1 - 2)} chemical reactivity and their interactions with HMIs (Zn^{2+}/Cd^{2+}/Hg^{2+}), respectively. The optimization of CNS, {$(NH_2)_n$-CNS (n = 1 - 2)}, and HMIs were carried out using a Gaussian software package (version 09) to obtain their low-lying structures (22). In the framework of quantum calculations, hybrid DFT methods, including the wB97XD exchange-correlation (xc) functional (23). with pseudopotential basis sets and lanl2dz, were used (24). Ground state with no imaginary frequencies was evaluated by frequency test. This work confirms that all structures are in actual minima. In addition, the molecular electrostatic potential (MEP) (25). was performed to better understand electronic structures and their role in reactions. For the investigation role of CNS, {$(NH_2)_n$-CNS (n = 1 - 2)}, and HMIs (Zn^{2+}/Cd^{2+}/Hg^{2+}) from seawater in interaction, their global and local descriptors were calculated in the DFT-based calculations.

Reactivity is the tendency to undergo a possible chemical reaction with other molecules (26). Global chemical reactivity descriptors are chemical potential (μ=$\frac{-(IE+EA)}{2}$), hardness (η=$\frac{IE-EA}{2}$), softness (S=$\frac{1}{\eta}$), and electrophilicity (ω=$\frac{\mu 2}{2\eta}$), respectively (26). In other words, the μ is the escaping tendency of electrons; the η is resistance to charge transfer; the ω is the floating of electron between nucleophile and electrophile (26). In these equations, the IE and EA are ionization energy and electron affinity according to the three approach points as follows: (26)

IE (compond) = E_{tot} (compound$^+$) - E_{tot} (compound)

EA (compound) = E_{tot} (compound$^-$) - E_{tot} (compound)

The active sites of CNS and {$(NH_2)_n$-CNS (n = 1 - 2)} for interaction with HMIs (Zn^{2+}/Cd^{2+}/Hg^{2+}) were predicted by the investigation of local descriptors, such as Fukui function (f) and local softness (s). The f is the sensitivity of the chemical potential of a system to a local external potential (26). Finite difference approximation was used to characterize nucleophilic (f^+) and electrophilic (f^-) attacks as follows: (26)

$$f_k^+ = q_k^{N+1} - q_k^N$$

$$f_k^- = q_k^N - q_k^{N-1}$$

Where q_k^N, q_k^{N+1}, and q_k^{N-1} are the electronic populations on selected atom a for the N, (N+1), and (N-1) electron systems, respectively. Local softness showed nucleophile (electrophile) site in a compound for electrophilic (nucleophilic) attacks as follows: (26)

$$s_k^\alpha = f_k^\alpha \times S$$

When α=+,- means nucleophilic, electrophilic attacks, the maximum positive values of local softness indicate most electrophile site of atom in the compound. Therefore, this site is favorable for nucleophilic attacks in reaction with other molecules.

The QTAIM (27) and NBO analysis (28) complete geometric and electronic information of zigzag CNS, {$(NH_2)_n$-CNS (n = 1 - 2)}, and HMIs (Zn^{2+}/Cd^{2+}/Hg^{2+}) interactions. Electron density ρ(r) and Laplacian $\nabla^2\rho$(r), electronic energy density H(r), electronic kinetic energy density G(r), and electronic potential energy density V(r) descriptors were calculated at bond critical points (BCPs) based on the QTAIM theory. Moreover, the type of bonds, depletion of occupancies, percentage of Lewis and nonLewis, and stabilization energies 28 were obtained by NBO analysis. The second-order stabilization energy (E_{ij}^2) of this interaction was calculated using the following equation:

$$E_{ij}^2 = \frac{\left| < i \left| \widehat{H} \right| j > \right|^2}{E_j - E_i} \quad (1)$$

Where $\widehat{H}$, E_j and E_i, and $< i \left| \widehat{H} \right| j >$ are interaction Hamiltonian, orbital energies, and matrix element, respectively.

4. Results and Discussion

Zigzag CNS and {$(NH_2)_n$-CNS (n = 1 - 2)} structures (CNS (n, m; L), and L equals to length (in angstrom, Å) are considered substrates for the adsorption and removal of

HMIs (Zn^{2+}/Cd^{2+}/Hg^{2+}) from seawater. The zigzag CNS and {$(NH_2)_n$-CNS (n = 1 - 2)} have chirality (10, 0) with 10 Å in length properties. The low lying structures of zigzag CNS and {$(NH_2)_n$-CNS (n = 1 - 2)} structures were investigated in the wB97/Lanl2dz level of theory (Figure 1). Symmetrical constraints (C1 symmetry) were not considered in optimization processing that leads to the exact investigation of ground states. On the other hand, frequency calculation confirmed this issue because there were no imaginary frequencies.

The investigation of active sites and the prediction of the strength of interactions in isolated {$(NH_2)_n$-CNS (n = 1 - 2)} structures were carried out using MEP maps (25) (Figure 2). Low and high electron density was related to the positive and negative points of charge distribution in the MEP map, respectively. The yellow, blue, and green colors elucidate the most negative, positive, and zero electrostatic potentials, respectively (Figure 2). According to Figure 2, adding one and/or two NH_2 groups mainly results in decreasing positive electrostatic potential in the center of CNS nanostructure. This issue confirms that the functionalization of CNS nanostructure can increase the chemical reactivity of this structure to interact with HMIs (Zn^{2+}/Cd^{2+}/Hg^{2+}).

The confirmation of the above-mentioned behavior of CNS and {$(NH_2)_n$-CNS (n = 1 - 2)} structures is understandable with the investigation of their role in the interaction. A simple way to achieve this purpose is using global chemical reactivity descriptors, as shown in Table 1. High and low negative values of the μ in HMIs (Zn^{2+}/Cd^{2+}/Hg^{2+}) and CNS, {$(NH_2)_n$-CNS (n = 1 - 2)}, indicated that they accept and donate electrons conveniently, respectively. Therefore, the HMIs (Zn^{2+}/Cd^{2+}/Hg^{2+}) and CNS, {$(NH_2)_n$-CNS (n = 1 - 2)}, NS play electrophile and nucleophile roles in their interaction. This issue is in line with the high η and low S of CNS and {$(NH_2)_n$-CNS (n = 1 - 2)} structures. Furthermore, the high ω of nucleophile showed that the floating of the electron was carried out from NSs to HMIs (Zn^{2+}/Cd^{2+}/Hg^{2+}) conveniently.

The local chemical reactivity method can help investigate the exact active sites of the NS in the interaction with HMIs (Zn^{2+}/Cd^{2+}/Hg^{2+}). According to Table 2, the local softness (s_N^-) of nitrogen atom sites have the most positive value in nucleophilic attacks. These active sites probably interact with HMIs (Zn^{2+}/Cd^{2+}/Hg^{2+}).

For more understanding of {$(NH_2)_n$-CNS (n = 1 - 2)} NSs and HMIs (Zn^{2+}/Cd^{2+}/Hg^{2+}) interaction, the highest occupied molecular orbital (HOMO) and lowest unoccupied molecular orbital (LUMO) have been plotted (Figure 3). According to Figure 3, the HOMO $(NH_2)_2$-CNS-LUMO HMI gap was decreased by about 1.35 eV more than the other NSs. Therefore, there is probably a strong charge transfer in HMIs → $(NH_2)_2$-CNS and $(NH_2)_2$-CNS → HMIs, respectively.

With the determination of the ground state of structures, the HMIs (Zn^{2+}/Cd^{2+}/Hg^{2+}) as ligand interacted with CNS and {$(NH_2)_n$-CNS (n = 1 - 2)} structures. The low lying structures of the open and closed-shell ({$(NH_2)_n$-CNS (n = 1 - 2)}- M^{2+} (M^{2+}= Zn^{2+}/Cd^{2+}/Hg^{2+}) complexes were investigated by the selected level of theory (Figure 4). The more negative value of the E^{ads} calculations implies that the $(NH_2)_2$-CNS-M^{2+} complexes have higher adsorption strength and stable configuration than the CNS- M^{2+} and (NH_2)-CNS-M^{2+} structures, as shown in Table 3. Therefore, the functionalized CNS structures have a tendency to interact with the HMIs. According to Table 3, the adsorption energy value in $(NH_2)_2$-CNS-Hg^{2+} is more than other complexes. This issue can be due to the interaction of two NH_2 groups with the HMIs.

4.1. QTAIM and NBO Analysis

The evaluation of the CNS… M^{2+} and {$(NH_2)_n$-CNS (n = 1 - 2)}… M^{2+} (M^{2+}= Zn^{2+}/Cd^{2+}/Hg^{2+}) interactions was carried out using QTAIM theory (27). Figure 5 depicts the bond paths (BPs) and BCPs of NSs and HMIs (M^{2+}= Zn^{2+}/Cd^{2+}/Hg^{2+}) interactions. According to Figure 5, there is no BP and BCPs in the CNS… M^{2+} systems. Table 4 shows the calculated descriptors at the BPs and BCPs of these interactions.

Probably the interactions in the CNS… M^{2+} systems are very weak. This issue is in line with E_{ads} calculations. Additionally, the information of the BCPs in the {$(NH_2)_n$-CNS (n = 1 - 2)}… M^{2+} confirms the interaction between functionalized NSs and HMIs. Therefore, the electron density values of ρ(r) in the BCP of this interaction were observed lower than the covalence bonds (Table 4). Moreover, the ρ(r) values decreased with an ascending trend in the atomic mass of HMIs and lowering distances in the $_2$HN…. M^{2+} interactions. This issue is in line with the elongation of the C–N bond. Therefore, high ρ(r), more elongation of the C–N bond, low $_2$HN… M^{2+} distance, and linearity of the M^{2+}…N-C angle lead to the charge transfer of nitrogen atom to HMIs. The small values of the $\nabla^2\rho$(r) and H(r) in $_2$HN…. M^{2+} indicated that the nature of these bonds is electrostatic. The positive and negative values of the $\nabla^2\rho$(r) in C–N, and $_2$HN…. M^{2+} bonds implied that these bonds have covalence and electrostatic natures. The high and low values of the H(r) descriptor in these bonds signified that the nature of such bonds was decreased and increased.

In spite of the fact that the QTAIM has high performance to investigate these types of interactions, it can-

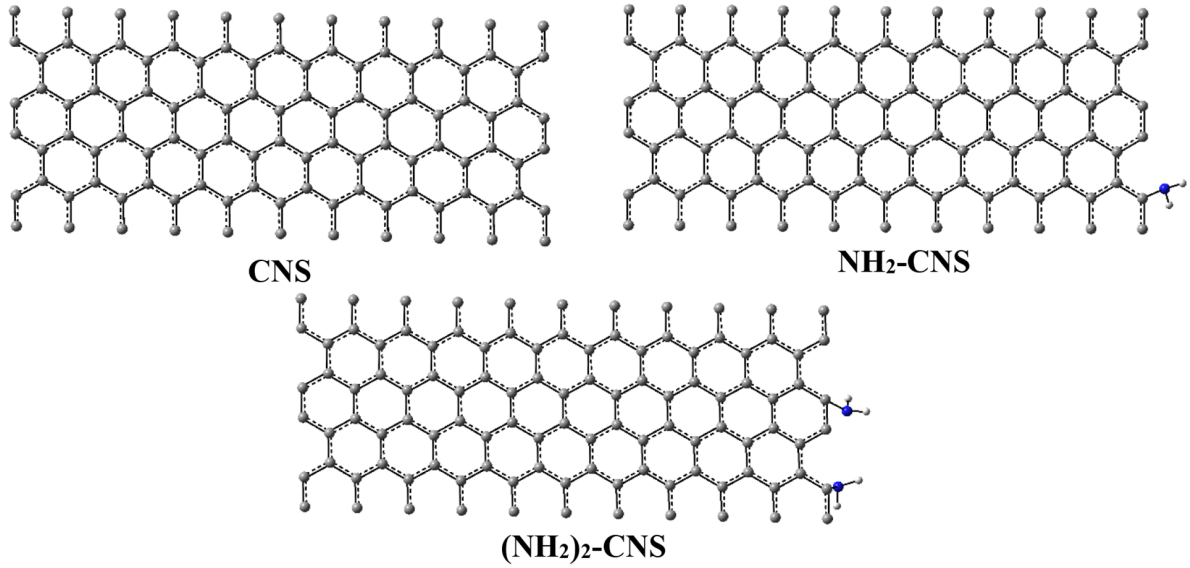

Figure 1. Optimal ground state structures of nanosheet structures in wB97XD/lanl2dz method

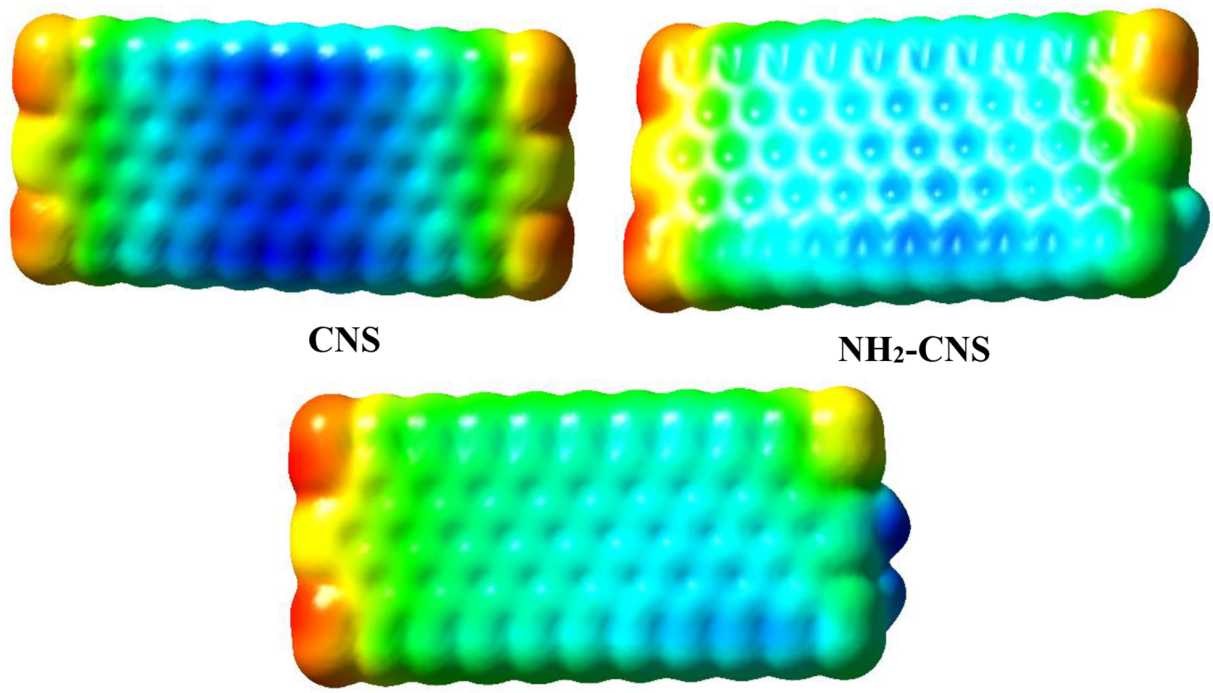

Figure 2. Calculated molecular electrostatic potential of nanosheet structures using wB97XD/lanl2dz method

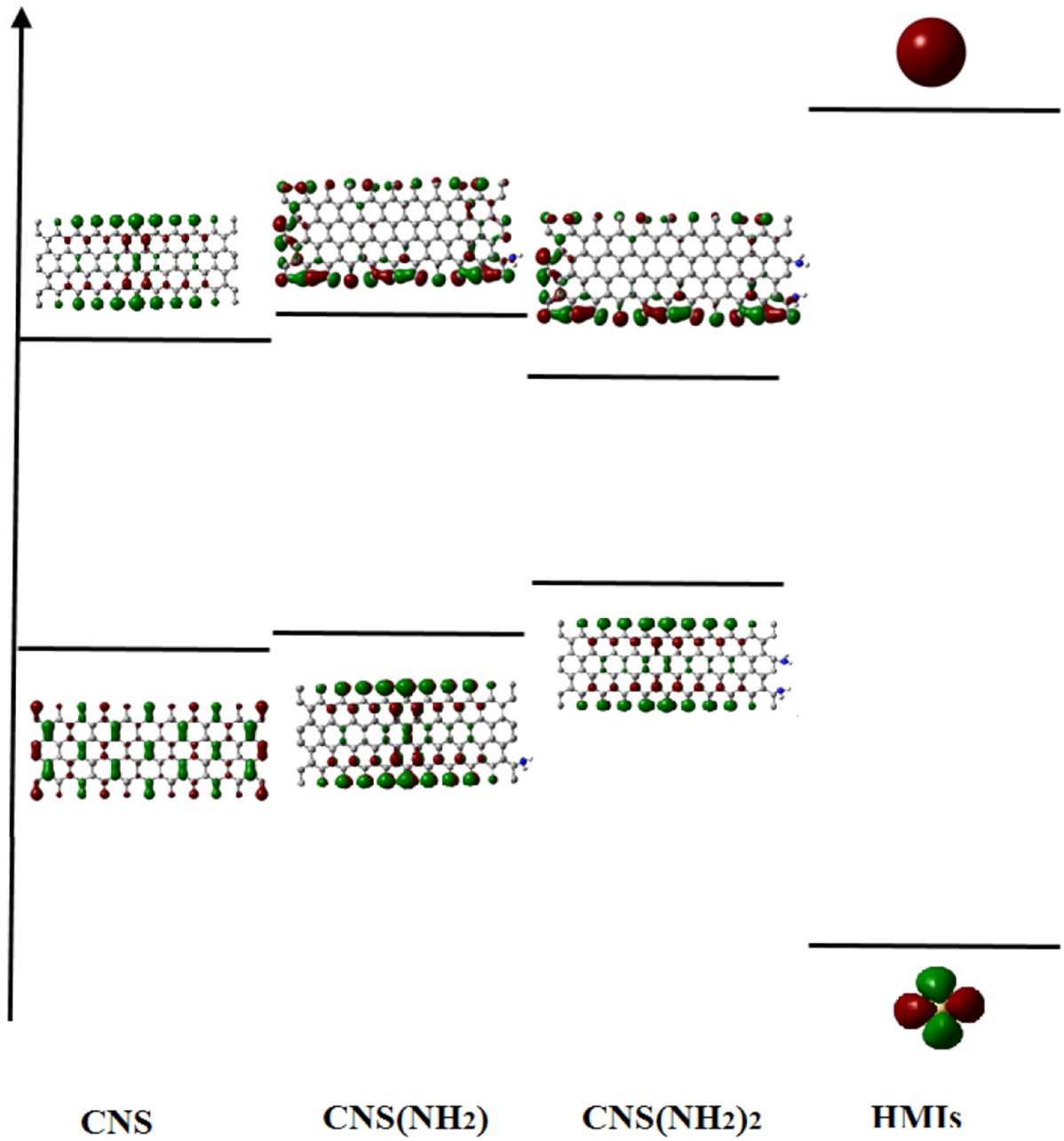

Figure 3. Highest Occupied molecular orbital and lowest unoccupied molecular orbital gaps of carbon nanosheet, {$(NH_2)_n$-CNS (n = 1 - 2)} structures, and heavy metal ions (Zn^{2+}/Cd^{2+}/Hg^{2+})

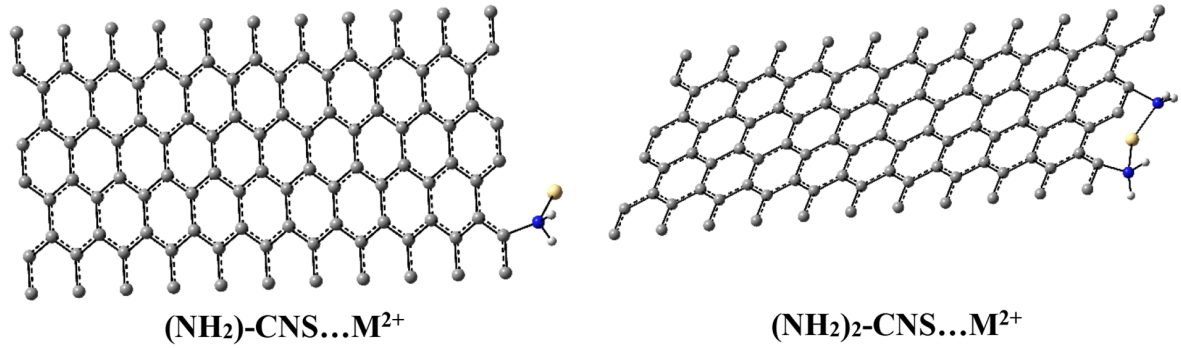

Figure 4. Optimized geometry of ({$(NH_2)_n$-carbon nanosheet (n = 1 - 2)}-M^{2+} (M^{2+} = Zn^{2+}/Cd^{2+}/Hg^{2+}) complexes at selected level of theory

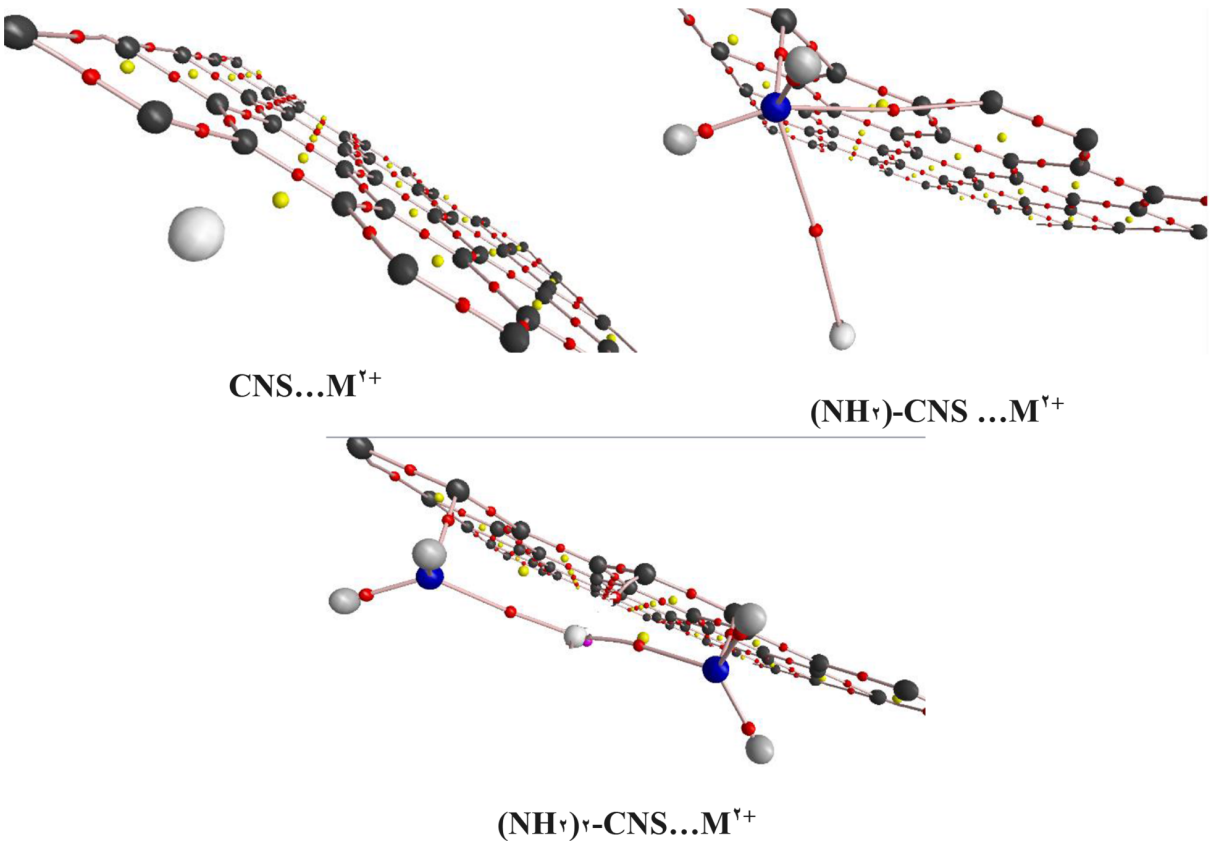

Figure 5. Molecular graph of carbon nanosheet (CNS)- M^{2+} and $(NH_2)_x$-CNS- M^{2+} (M= Zn^{2+}, Cd^{2+}, Hg^{2+}, x = 1 - 2); Bond critical point (in red) and ring critical point (in yellow)

Table 1. Ionization Energy, Electron Affinity, Chemical Potential (μ), Global Hardness (η), Softness (S), and Electrophilicity (ω) of Carbon Nanosheet, {$(NH_2)_n$-CNS (n = 1 - 2)}, and Heavy Metal Ions, Respectively

Descriptors (eV)	CNS	(NH_2)-CNS	$(NH_2)_2$-CNS	Zn^{2+}	Cd^{2+}	Hg^{2+}
IE	3.005	2.8148	2.8639	28.8148	32.0089	29.9731
EA	0.5648	0.2276	0.7892	20.4476	19.4673	20.9037
μ	-1.7851	-1.5212	-1.8266	-24.6312	-25.7381	-25.4384
η	1.2203	1.2936	1.0373	4.1836	6.2708	4.5347
S	0.8195	0.7731	0.9640	0.2390	0.1595	0.2205
ω	1.3057	0.8944	1.6081	72.5095	52.8201	71.3510

Abbreviations: IE, ionization energy; EA, electron affinity; CNS, carbon nanosheet.

Table 2. Calculated Local Descriptors of {$(NH_2)_n$-CNS (n = 1 - 2)} Structures in Selected Level of Theory

Atoms	f^+	f^-	s^+	s^-
C	0.01651	-0.01505	0.01592	-0.01450
N	0.00417	-0.00396	0.00402	-0.00381

Table 3. Calculated Adsorption Energies of Carbon Nanosheet (CNS) and $CNS(NH_2)_n$ (n = 1 - 2)… M^{2+} Complexes in wB97XD/lanl2dz Method

Complexes	Zn	Cd	Hg
CNS	-4.31	-3.09	-7.43
CNS (NH_2)	-10.27	-13.34	-17.43
CNS $(NH_2)_2$	-75.72	-84.39	-93.48

Abbreviation: CNS, carbon nanosheet.

not identify the source of changes and charge transfers (27). Therefore, NBO analysis (28) showed that there are two significant donor-acceptor interactions in the {$(NH_2)_n$-CNS (n = 1 - 2)}… M^{2+} systems, such as $nN \rightarrow lp^*M^{2+}$ and $lpM^{2+} \rightarrow \sigma^*C\text{–}N$, with the second-order stabilization energies of 65.8 and 13.01 kcal mol^{-1}, respectively. Consequently, $nN \rightarrow lp^*M^{2+}$ interaction was stronger than $lpM^{2+} \rightarrow \sigma^*C\text{–}N$, which is in line with QTAIM analysis.

5. Conclusions

The CNS structures can help to the removal of HMIs (Zn^{2+}/Cd^{2+}/Hg^{2+}) from water, especially seawater and/or wastewater. For the achievement of this purpose, CNS and amine-functionalized NS ({$(NH_2)_n$-CNS (n = 1 - 2)}) interacted with HMIs (Zn^{2+}/Cd^{2+}/Hg^{2+}). Based on DFT, $(NH_2)_2$-CNS has a good ability for the removal of HMIs due to high chemical potential (-1.827 eV), softness (0.964 eV), high electrophilicity (1.608 eV), and adsorption energy (≈ -75 to -93 kJ mol^{-1}) in the $(NH_2)_2$-CNS… M^{2+} complex. The aforementioned issues are confirmed by donor-acceptor interactions and strongly formed BCPs based on NBO and QTAIM methodologies.

Acknowledgments

The authors would like to express their gratitude to Dr. Fazlolah Eshghi for his helpful suggestions concerning this study.

Footnotes

Authors' Contribution: Dr. Amir Hessam Hasani conceived the presented idea. Mrs. Hossein Laila Javarani developed the theory, performed the computations, directed the project, suggested the probable mechanism, and edited and revised the manuscript. Dr. Mohammad Malakootian and Amir Hossein Javid wrote the manuscript. All the authors discussed the results and contributed to the final manuscript.

Conflict of Interests: There is no conflict of interest.

Data Reproducibility: The data presented in this study are openly available in one of the repositories or will be available on request from the corresponding author by this journal representative at any time during submission or after publication. Otherwise, all the consequences of possible withdrawal or future retraction will be with the corresponding author.

Table 4. Analysis of Bond Critical Points in Covalence and Electrostatic Bonds at $(NH_2)_n$-CNS... M^{2+} (n = 1 - 2) Complexes

Complexes, Bond	$\rho(\mathbf{r})$	$\nabla^2\rho(\mathbf{r})$	H(r)
(NH_2)-CNS- Zn^{2+}			
C-N	0.2378	0.10160	0.197717
N-Zn^{2+}	0.01816	-0.01313	0.000449
(NH_2)-CNS-Cd^{2+}			
C-N	0.1704	0.12960	0.176100
N-Cd^{2+}	0.0171	-0.01498	0.000762
(NH_2)-CNS-Hg^{2+}			
C-N	0.2181	0.10260	0.16043
N-Hg^{2+}	0.01795	-0.01342	0.000726
$(NH_2)_2$-CNS-Zn^{2+}			
C-N left	0.2252	0.08507	0.21998
C-N right	0.2346	0.09714	0.20867
N-Zn^{2+} left	0.08971	-0.10277	0.023108
N-Zn^{2+} right	0.09731	-0.11368	0.026925
$(NH_2)_2$-CNS-Cd^{2+}			
C-N	0.1159	0.09370	0.23007
C-N	0.1250	0.1027	0.21803
N-Cd^{2+}	0.08243	-0.10781	0.03169
N-Cd^{2+}	0.07510	-0.11627	0.031015
$(NH_2)_2$-CNS-Hg^{2+}			
C-N	0.13261	0.09104	0.16181
C-N	0.13038	0.09539	0.15882
N-Hg^{2+}	0.09224	-0.11020	0.04021
N-Hg^{2+}	0.09268	-0.12053	0.04537

Funding/Support: This study was carried out with a personal fund.

References

1. Hamed Mashhadzadeh A, Fathalian M, Ghorbanzadeh Ahangari M, Shahavi MH. DFT study of Ni, Cu, Cd and Ag heavy metal atom adsorption onto the surface of the zinc-oxide nanotube and zinc-oxide graphene-like structure. *Mater Chem Phys*. 2018;**220**:366–73. doi: 10.1016/j.matchemphys.2018.09.016.
2. Li J, Jin P, Dai W, Wang C, Li R, Wu T, et al. Excellent performance for water purification achieved by activated porous boron nitride nanosheets. *Mater Chem Phys*. 2017;**196**:186–93. doi: 10.1016/j.matchemphys.2017.02.049.
3. Liu F, Yu J, Ji X, Qian M. Nanosheet-structured boron nitride spheres with a versatile adsorption capacity for water cleaning. *ACS Appl Mater Interfaces*. 2015;**7**(3):1824–32. doi: 10.1021/am507491z. [PubMed: 25552343].
4. Li Q, Liu Y, Yu X, Li L, Zhang X, Lu Z, et al. Removal of Cr(iii)/Cr(vi) from wastewater using defective porous boron nitride: a DFT study. *Inorg Chem Front*. 2018;**5**(8):1933–40. doi: 10.1039/c8qi00416a.
5. Azamat J, Khataee A, Joo SW. Separation of copper and mercury as heavy metals from aqueous solution using functionalized boron nitride nanosheets: A theoretical study. *J Mol Struct*. 2016;**1108**:144–9. doi: 10.1016/j.molstruc.2015.11.058.
6. Nhantumbo C, Larsson R, Larson M, Juízo D, Persson K. A Simplified Model to Estimate the Concentration of Inorganic Ions and Heavy Metals in Rivers. *Water*. 2016;**8**(10). doi: 10.3390/w8100453.
7. Kommu A, Singh JK. A review on graphene-based materials for removal of toxic pollutants from wastewater. *Soft Materials*. 2020;**18**(2-3):297–322. doi: 10.1080/1539445x.2020.1739710.
8. Cao Y, Li X. Adsorption of graphene for the removal of inorganic pollutants in water purification: a review. *Adsorption*. 2014;**20**(5-6):713–27. doi: 10.1007/s10450-014-9615-y.
9. Wang S, Sun H, Ang HM, Tadé MO. Adsorptive remediation of environmental pollutants using novel graphene-based nanomaterials. *Chem Eng J*. 2013;**226**:336–47. doi: 10.1016/j.cej.2013.04.070.
10. Wang X, Chen Z, Yang S. Application of graphene oxides for the removal of Pb(II) ions from aqueous solutions: Experimental and DFT calculation. *J Mol Liq*. 2015;**211**:957–64. doi: 10.1016/j.molliq.2015.08.020.
11. Yu G, Lu Y, Guo J, Patel M, Bafana A, Wang X, et al. Carbon nanotubes, graphene, and their derivatives for heavy metal removal. *Adv Compos Hybrid Mater*. 2017;**1**(1):56–78. doi: 10.1007/s42114-017-0004-3.
12. Wu Y, Pang H, Liu Y, Wang X, Yu S, Fu D, et al. Environmental remediation of heavy metal ions by novel-nanomaterials: A review. *Environ Pollut*. 2019;**246**:608–20. doi: 10.1016/j.envpol.2018.12.076. [PubMed: 30605816].
13. Mahmoud KA, Mansoor B, Mansour A, Khraisheh M. Functional graphene nanosheets: The next generation membranes for water desalination. *Desalination*. 2015;**356**:208–25. doi: 10.1016/j.desal.2014.10.022.
14. Elgengehi SM, El-Taher S, Ibrahim MA, Desmarais JK, El-Kelany KE. Graphene and graphene oxide as adsorbents for cadmium and lead heavy metals: A theoretical investigation. *Appl Surf Sci*. 2020;**507**. doi: 10.1016/j.apsusc.2019.145038.
15. Yu JG, Yu LY, Yang H, Liu Q, Chen XH, Jiang XY, et al. Graphene nanosheets as novel adsorbents in adsorption, preconcentration and removal of gases, organic compounds and metal ions. *Sci Total Environ*. 2015;**502**:70–9. doi: 10.1016/j.scitotenv.2014.08.077. [PubMed: 25244035].
16. Liu X, Ma R, Wang X, Ma Y, Yang Y, Zhuang L, et al. Graphene oxide-based materials for efficient removal of heavy metal ions from aqueous solution: A review. *Environ Pollut*. 2019;**252**(Pt A):62–73. doi: 10.1016/j.envpol.2019.05.050. [PubMed: 31146239].
17. Li Y, Xu Z, Liu S, Zhang J, Yang X. Molecular simulation of reverse osmosis for heavy metal ions using functionalized nanoporous graphenes. *Comput Mater Sci*. 2017;**139**:65–74. doi: 10.1016/j.commatsci.2017.07.032.
18. Khulbe KC, Matsuura T. Removal of heavy metals and pollutants by membrane adsorption techniques. *Appl Water Sci*. 2018;**8**(1). doi: 10.1007/s13201-018-0661-6.
19. Li Z, Chen F, Yuan L, Liu Y, Zhao Y, Chai Z, et al. Uranium(VI) adsorption on graphene oxide nanosheets from aqueous solutions. *Chem Eng J*. 2012;**210**:539–46. doi: 10.1016/j.cej.2012.09.030.
20. Huang H, Chen T, Liu X, Ma H. Ultrasensitive and simultaneous detection of heavy metal ions based on three-dimensional graphene-carbon nanotubes hybrid electrode materials. *Anal Chim Acta*. 2014;**852**:45–54. doi: 10.1016/j.aca.2014.09.010. [PubMed: 25441878].
21. Wang J, Zhang J, Han L, Wang J, Zhu L, Zeng H. Graphene-based materials for adsorptive removal of pollutants from water and underlying interaction mechanism. *Adv Colloid Interface Sci*. 2021;**289**:102360. doi: 10.1016/j.cis.2021.102360. [PubMed: 33540288].

22. Frisch G, Trucks H, Schlegel GM, Robb J, Cheeseman G, Scalmani V, et al. *Gaussian 09, Revision A.1*. Wallingford, CT: Gaussian, Inc; 2009.
23. Chai JD, Head-Gordon M. Long-range corrected hybrid density functionals with damped atom-atom dispersion corrections. *Phys Chem Chem Phys*. 2008;**10**(44):6615–20. doi: 10.1039/b810189b. [PubMed: 18989472].
24. Dunning Jr TH. *Modern Theoretical Chemistry*. New York, USA: Plenum; 1976.
25. Tasi G, Palinko I, Nyerges L, Fejes P, Foerster H. Calculation of electrostatic potential maps and atomic charges for large molecules. *J Chem Inf Comput Sci*. 1993;**33**(3):296–9. doi: 10.1021/ci00013a003.
26. Parr RG, Yang W. Density functional theory of atoms and molecules. *Oxford Univ Press*. 1989;**1**:1989.
27. Bader RFW, Nguyen-Dang TT, Tal Y. A topological theory of molecular structure. *Rep Prog Phys*. 1981;**44**(8):893–948. doi: 10.1088/0034-4885/44/8/002.
28. Reed AE, Weinstock RB, Weinhold F. Natural population analysis. *J Chem Phys*. 1985;**83**(2):735–46. doi: 10.1063/1.449486.